

# Lactate-Mediated Acidification of Tumor Microenvironment Induces Apoptosis of Liver-Resident NK Cells in Colorectal Liver Metastasis



Cathal Harmon<sup>1</sup>, Mark W. Robinson<sup>1,2</sup>, Fiona Hand<sup>1,3</sup>, Dalal Almuaili<sup>1</sup>, Keno Mentor<sup>3</sup>, Diarmaid D. Houlihan<sup>3</sup>, Emir Hoti<sup>3</sup>, Lydia Lynch<sup>1,4</sup>, Justin Geoghegan<sup>3</sup>, and Cliona O'Farrelly<sup>1,2</sup>

## Abstract

Colorectal cancer is the third most common malignancy worldwide, with 1.3 million new cases annually. Metastasis to the liver is a leading cause of mortality in these patients. In human liver, metastatic cancer cells must evade populations of liver-resident natural killer (NK) cells with potent cytotoxic capabilities. Here, we investigated how these tumors evade liver NK-cell surveillance. Tissue biopsies were obtained from patients undergoing resection of colorectal liver metastasis (CRLM,  $n = 18$ ), from the tumor, adjacent tissue, and distal resection margin. The number and phenotype of liver-resident NK cells, at each site, were analyzed by flow cytometry. Tumor-conditioned media (TCM) was generated for cytokine and metabolite quantification and used to treat healthy liver-resident NK cells, isolated from donor liver perfusate during transplantation. Liver-resident NK cells were significantly

depleted from CRLM tumors. Healthy liver-resident NK cells exposed to TCM underwent apoptosis *in vitro*, associated with elevated lactate. Tumor-infiltrating liver-resident NK cells showed signs of mitochondrial stress, which was recapitulated *in vitro* by treating liver-resident NK cells with lactic acid. Lactic acid induced apoptosis by decreasing the intracellular pH of NK cells, resulting in mitochondrial dysfunction that could be prevented by blocking mitochondrial ROS accumulation. CRLM tumors produced lactate, thus decreasing the pH of the tumor microenvironment. Liver-resident NK cells migrating toward the tumor were unable to regulate intracellular pH resulting in mitochondrial stress and apoptosis. Targeting CRLM metabolism provides a promising therapeutic approach to restoring local NK-cell activity and preventing tumor growth.

## Introduction

Colorectal cancer represents a major health problem worldwide, with more than 1.3 million new cases per year (1). Advancing age of populations globally and rising rate of obesity are driving increasing rates of colorectal cancer (2). Metastasis is a major cause of morbidity and mortality in colorectal cancer patients. In the absence of distant metastases (stages I–III), 5-year survival ranges between 70% and 90%; however, in patients with metastatic disease (stage IV), this is only 14% (3). The liver is the most common site of distant metastasis, with up to 50% of patients developing colorectal liver metastasis (CRLM; refs. 4, 5). However, it remains unknown how metastatic colorectal cells colonize an immunocompetent organ and avoid local immunosurveillance.

The adult human liver contains an extensive repertoire of antitumor immune cells. Innate lymphoid cells, including natural killer (NK) cells, natural killer T (NKT) cells, mucosal associated invariant T (MAIT) cells, and  $\gamma\delta$  T cells, predominate in the liver. Conventional CD4<sup>+</sup> and CD8<sup>+</sup> T cells are also present, with an increased proportion of cytotoxic CD8<sup>+</sup> T cells (6–11). NK cells are group 1 innate lymphoid cells (ILC), important in antiviral and tumor immunity, and in particular the control of metastasis (12), with NK-cell therapies currently being trialed for the treatment of CRLM (13). The human liver contains resident NK cells possessing enhanced antitumor activity characterized by increased degranulation (14–16). These cells are characterized as CD56<sup>bright</sup> NK cells, express the chemokine receptor CXCR6, and have a unique transcription factor profile (Eomes<sup>hi</sup>Tbet<sup>lo</sup>).

The evidence that immune infiltration of colorectal cancer is a determinant of disease outcome has led to the development of the Immunoscore as a routine diagnostic test (17–19). The density of T- and NK-cell infiltration of CRLM tumors has been shown to positively predict survival (20). However, infiltration of T and NK cells was highly variable, and some tumors were almost devoid of NK cells. NK cells appear to play a central role in the outcome of CRLM, demonstrated by their depletion and compromised function in primary colorectal cancer tumors and blood (21, 22). It remains unknown whether liver-resident NK cells are dysfunctional in metastases to the liver. We believe this loss of immunosurveillance is in part driven by the unique tumor microenvironment. The liver microenvironment is dramatically altered in the presence of CRLM (23–25), and the metabolic changes

<sup>1</sup>School of Biochemistry and Immunology, Trinity Biomedical Sciences Institute, Trinity College Dublin, Dublin, Ireland. <sup>2</sup>School of Medicine, Trinity College Dublin, Dublin, Ireland. <sup>3</sup>Liver Unit, St. Vincent's University Hospital, Dublin, Ireland. <sup>4</sup>Department of Medicine, Brigham and Women's Hospital, Harvard Medical School, Boston, Massachusetts.

**Note:** Supplementary data for this article are available at Cancer Immunology Research Online (<http://cancerimmunolres.aacrjournals.org/>).

**Corresponding Author:** Cliona O'Farrelly, Trinity College Dublin, Dublin, D02 R590, Ireland. Phone: 353-1896-3175; Fax: 353-1677-2400; E-mail: OFARRECL@tcd.ie

doi: 10.1158/2326-6066.CIR-18-0481

©2018 American Association for Cancer Research.

Harmon et al.

associated with tumor growth can have profound effects on infiltrating immune cells, especially T and NK cells, which require metabolic reprogramming upon activation (26–29).

In this study, we have characterized the distribution of liver-resident NK cells in different regions of tumor-bearing liver, tumor, tumor adjacent, and distal tissue from the resection margin. Using *in vitro* culture techniques, generating conditioned media from tumor and healthy tissue, we have identified lactate, a metabolite of glycolysis, which induces the apoptosis of liver-resident NK cells. This pathway provides the rationale for potential therapeutic approaches for the reinvigoration of liver-resident NK cells to limit CRLM growth.

## Materials and Methods

### Patient recruitment

Patients attending the National Liver Unit at St. Vincent's University Hospital for hepatic metastasectomy secondary to tumors of colorectal origin were eligible for inclusion in this study. Eighteen patients were recruited preoperatively (Table 1). Donor liver biopsies and liver perfusate (LP) samples were collected during orthotopic liver transplantation ( $n = 17$ ; Table 1). All patients provided written informed consent. This study was carried out in accordance with the Declaration of Helsinki and was reviewed and approved by the ethics committee of St. Vincent's University Hospital.

### Isolation of hepatic mononuclear cells from liver perfusate, liver biopsy, and peripheral blood

Hepatic mononuclear cells (HMNCs) were isolated from donor LP, as previously described (14, 30). Briefly, exsanguinated donor livers were flushed and immersed in University of Wisconsin solution for transport (transport medium). In theater, the donor liver was flushed with saline to remove remaining transport medium (flush). The transport medium and flush are combined to make up the liver perfusate. HMNCs were then isolated by density centrifugation after filtration of perfusate. HMNCs were isolated from biopsies from tumor, tumor adjacent, and distal

tissue from hepatic resection for CRLM, by mechanical and enzymatic digestion (collagenase type V, Sigma-Aldrich), as previously described (31).

### Preparation of liver-conditioned media

Donor liver biopsies and CRLM tumors were used to generate tissue-conditioned media (CM) as previously described (24, 32). Tissue was cut into sections approximately 5 mm<sup>3</sup> and incubated in 500  $\mu$ L of RPMI-1640, with 10% fetal calf serum and 1% penicillin/streptomycin (Gibco) for 72 hours at 37°C. The supernatant was centrifuged to remove cell debris and stored at –80°C until use.

### Phenotypic analysis of NK cells

HMNCs ( $1 \times 10^5$ ) were stained in FACS buffer for 30 minutes in the dark with fluorescently labeled monoclonal antibodies to determine the phenotypic differences between hepatic NK cells. A full list of antibodies used can be found in Supplementary Table S1. Dead cell exclusion was performed using fixable viability stain 780 (BD Biosciences). Mitochondrial mass was assessed using MitoTracker Deep Red (Thermo Fisher); mitochondrial ROS production was measured using MitoSox (Thermo Fisher). Flow cytometry analysis was performed using an LSRFortessa, using fluorescence-minus-one controls (FMO; BD Biosciences), and data were analyzed using FlowJo (Version 7.6.5, Tree Star).

### Isolation of NK-cell subset from liver perfusate

NK cells were isolated from fresh LP by FACS. Briefly, donor LP was stained with monoclonal antibodies. NK cells were sorted into two populations CD56<sup>bright</sup> CD16<sup>+/-</sup> and CD56<sup>dim</sup> CD16<sup>++</sup> using a FACSAria cell sorter (BD Biosciences).

### Quantitative PCR

Total RNA was extracted from FACS-sorted NK cells from LP and tissue from tumor and healthy tissue, using TRIzol reagent (Thermo Fisher). Reverse transcription was performed using the SuperScript VILO Master Mix (Thermo Fisher). Quantitative PCR was performed using primers for *SLC16A1*, *SLC16A3*, and *SLC2A1* (see Supplementary Table S1 for primer sequences) using the PowerUp SYBR Green Master Mix (Thermo Fisher) on a StepOnePlus Real-Time PCR System (Thermo Fisher). *RPS15* and *B2M* were used as reference genes to generate normalized relative expression values for target genes.

### Cell line maintenance

The K562 and SW620 cell lines were purchased from ATCC between 2008 and 2010. Experiments were performed on cells less than 15 passages from purchase. Cells were routinely tested for contamination using the LookOut Mycoplasma PCR Detection Kit (Sigma-Aldrich). Cell identity of 168 SW620 was performed by IdentiCell (Denmark). Cell identity of K562 cells has not been performed.

### Cytotoxicity assay

Target cells (K562 or SW620) were labeled with CellTrace Violet (CTV). FACS-sorted liver NK cells were incubated with target cells at a ratio of 2:1 for 4 hours. Anti-CD107a was added to assess degranulation. Cytotoxicity was assessed by propidium iodide staining (PI). CTV<sup>+</sup> cells were gated, and PI<sup>+</sup> cells were measured as a percentage of target cells.

**Table 1.** Patient and organ donor demographics

CRLM patients	N = 18
Sex	
Male (%)	12 (66)
Female (%)	6 (33)
Age	
Median (range)	65 (50–79)
Number of liver metastases	
Median (range)	2 (1–5)
Tumor size (mm)	
Median (range)	22.5 (7–100)
Timing of CRLM	
Synchronous	10
Metasynchronous	8
Neoadjuvant chemotherapy (%)	12 (66)
Disease recurrence, n= (%)	
Yes	4 (22)
No	14 (78)
Organ donor	N = 17
Sex	
Male	9
Female	8
Age	
Median (range)	49 (28–67)

### Chemotaxis assay

Chemotaxis of liver NK cells was assessed using transwell inserts. Briefly, the lower chamber of the well was filled with serum-free RPMI-1640 media supplemented with 10% v/v CM. Liver NK cells ( $1 \times 10^5$ ) were applied to the upper chamber. Plates were incubated for 2 hours at 37°C. Cell numbers were assessed by flow cytometry using 123Count eBeads (eBiosciences) to enumerate absolute cell counts.

### Apoptosis assay

Apoptosis was assessed by annexin V/7-AAD staining. After treatment, NK cells were placed in annexin staining buffer and incubated for 20 minutes at RT with 2  $\mu$ L annexin V. After washing, 1  $\mu$ L 7-AAD was added to each tube before acquisition on flow cytometer. Apoptotic cells were defined as annexin V<sup>+</sup> 7AAD<sup>+</sup>. Caspase 8 activity was blocked in experiments using Z-IETD-FMK (BD Biosciences). Cells were treated with Z-IETD-FMK (50  $\mu$ mol/L) for 2 hours before the addition of TCM for 24 hours.  $\alpha$ -Cyano-4-hydroxycinnamic acid ( $\alpha$ CHC, Sigma-Aldrich) was used to block lactate transport.  $\alpha$ CHC (500  $\mu$ mol/L) was administered for 2 hours before the addition of TCM for 24 hours. MitoTempo (Sigma-Aldrich), a mitochondrial ROS scavenger, was used in further experiments. Cells were treated with MitoTempo (50  $\mu$ mol/L) for 2 hours before the addition of TCM for either 2 or 24 hours.

### Measurement of metabolites

Lactate concentrations were analyzed using a colorimetric enzymatic assay (Sigma-Aldrich). The lactate determination kit comes with premade lactate assay buffer, lactate probe, enzyme mix, and standards. Samples were prepared and analyzed as per the manufacturer's protocol. Briefly, CM samples were diluted 1:50 in lactate assay buffer. Sample (50  $\mu$ L) was incubated with 50  $\mu$ L reaction mixture for 30 minutes at RT. Absorbance was measured at 570 nm. Similarly, glucose concentrations were measured using an enzymatic assay as per the manufacturer's instructions (Abcam). Conditioned media were diluted 1:50 in glucose assay buffer and incubated with an equal volume of reaction buffer, at 37°C for 30 minutes. Absorbance was measured at 570 nm.

### Intracellular pH measurement

Intracellular pH was measured using the pH sensitive dye pHrodo (Thermo Fisher). This compound is retained within the cytosol and becomes increasingly fluorescent as pH decreases. Fluorescence was measured using flow cytometry. Controls were established by treating NK cells with buffers of pH 7.5, 6.5, and 5.5.

### Intracellular ATP measurement

Intracellular ATP was measured by luciferase assay (Invitrogen). After treatment, NK cells were lysed using DTT buffer. A luciferase construct, requiring ATP for activity, was used to determine intracellular ATP concentrations. Luminescence was measured using Fluoroskan Ascent FL (Labsystems).

### ELISA

IL15 concentrations in CM were measured by ELISA according to the manufacturer's instructions (PeproTech).

### Statistical analysis

Statistical analysis was carried out using Prism GraphPad Version 5.0. For comparison of two unmatched groups, Mann-Whitney *U* test was used. Comparison of more than two unmatched groups was performed using Kruskal-Wallis test, with Dunn multiple comparison test. For paired comparisons, Friedman test with Dunn multiple comparison tests was used for more than two groups, and Wilcoxon signed rank test was used for comparison of two matched groups. Within an experiment, \*, \*\* and \*\*\* represent  $P < 0.05$ ,  $P < 0.01$ , and  $P < 0.001$ , respectively.

## Results

### Liver-resident NK cells are depleted from colorectal liver metastasis tumors

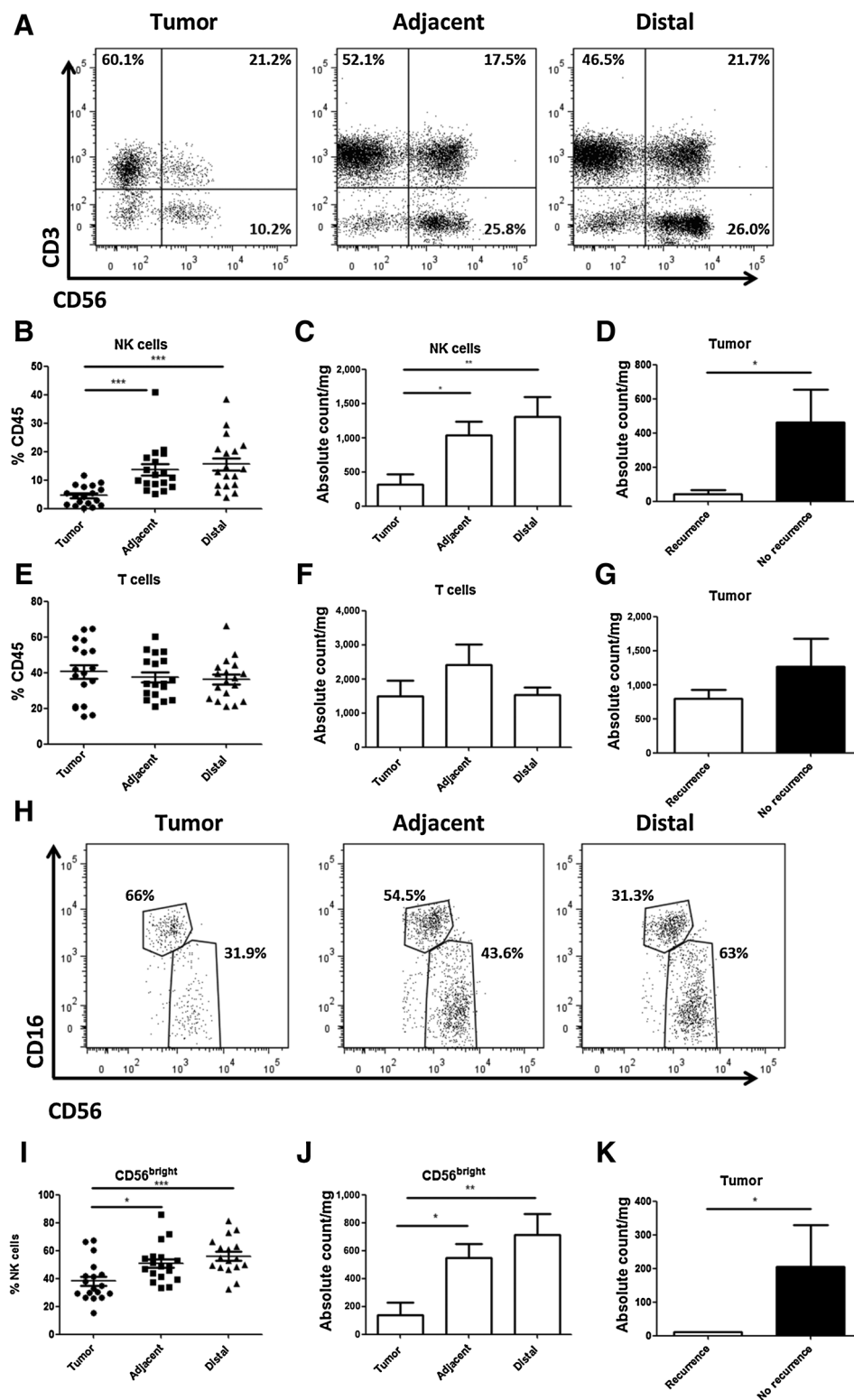
We have investigated the presence of liver-resident CD56<sup>bright</sup> NK cells in CRLM tumors and surrounding tissue. NK cells are significantly reduced in CRLM tumors (tumor 4.5%  $\pm$  0.8%, adjacent 13.6%  $\pm$  1.9%, distal 15.6%  $\pm$  2.2%,  $P < 0.0001$ ; Fig. 1A-C). Patients with recurrent hepatic disease had significantly lower intratumoral NK-cell numbers (recurrence: 41.2  $\pm$  24.1/mg, no recurrence: 460.7  $\pm$  193.0/mg,  $P = 0.047$ ; Fig. 1D). T cells appear unaffected in CRLM, with no significant difference in the population number throughout the tumor-bearing organ (Fig. 1E and F). No correlation between T-cell infiltration of the tumor and disease recurrence was observed (Fig. 1G). The largest reduction in NK cells was seen from the liver-resident CD56<sup>bright</sup> population (tumor 38.1%  $\pm$  3.4%, adjacent 50.8%  $\pm$  3.2%, distal 56.0%  $\pm$  3.2%,  $P = 0.0009$ ; Fig. 1H-J). This depletion of liver-resident CD56<sup>bright</sup> NK cells was significantly worse in patients who went on to develop recurrent CRLM (recurrence: 10.4  $\pm$  1.3/mg, no recurrence: 204.7  $\pm$  124.2/mg,  $P = 0.0238$ ; Fig. 1K).

Liver-resident NK cells display an activated phenotype compared with conventional CD56<sup>dim</sup> cells isolated from liver perfusate. They display increased expression of activation markers, including NKG2D, NKp46, and NKp44 (Supplementary Fig. S1A-F). They express cytotoxic molecules such as perforin, granzyme B, granzyme A, and granzyme K (Supplementary Fig. S1G-K). Despite lower expression of granzyme B and perforin compared with CD56<sup>dim</sup> NK cells from liver perfusate, liver-resident CD56<sup>bright</sup> NK cells degranulate significantly more in response to tumor cells and are capable of direct cytotoxicity against the metastatic colorectal cell line SW620, equal to CD56<sup>dim</sup> NK cells (Supplementary Fig. S1L-O).

### Tumor-infiltrating CD56<sup>bright</sup> NK cells have liver-resident phenotype

The remaining CD56<sup>bright</sup> NK cells maintained a tissue-resident phenotype (Eomes<sup>hi</sup> Tbet<sup>lo</sup>; Fig. 2A and B) throughout the tumor-bearing tissue. In addition, they maintained expression of other markers of tissue residency, including CXCR6, CD69, CD49a, and TRAIL (Fig. 2C-G). This indicated that CD56<sup>bright</sup> NK cells were not infiltrating peripheral blood cells and that liver-resident NK cells throughout the liver may be activated in CRLM. A decrease in the absolute count of CD56<sup>dim</sup> NK cells was also observed in the tumor; however, the scale of this change was smaller than liver-resident NK cells (Supplementary Fig. S2A-C). The remaining CD56<sup>dim</sup> cells were Eomes<sup>lo</sup> Tbet<sup>hi</sup> and failed to highly express markers of tissue residency, CXCR6, CD69, and CD49a. However, they did express TRAIL, which may indicate an activated phenotype

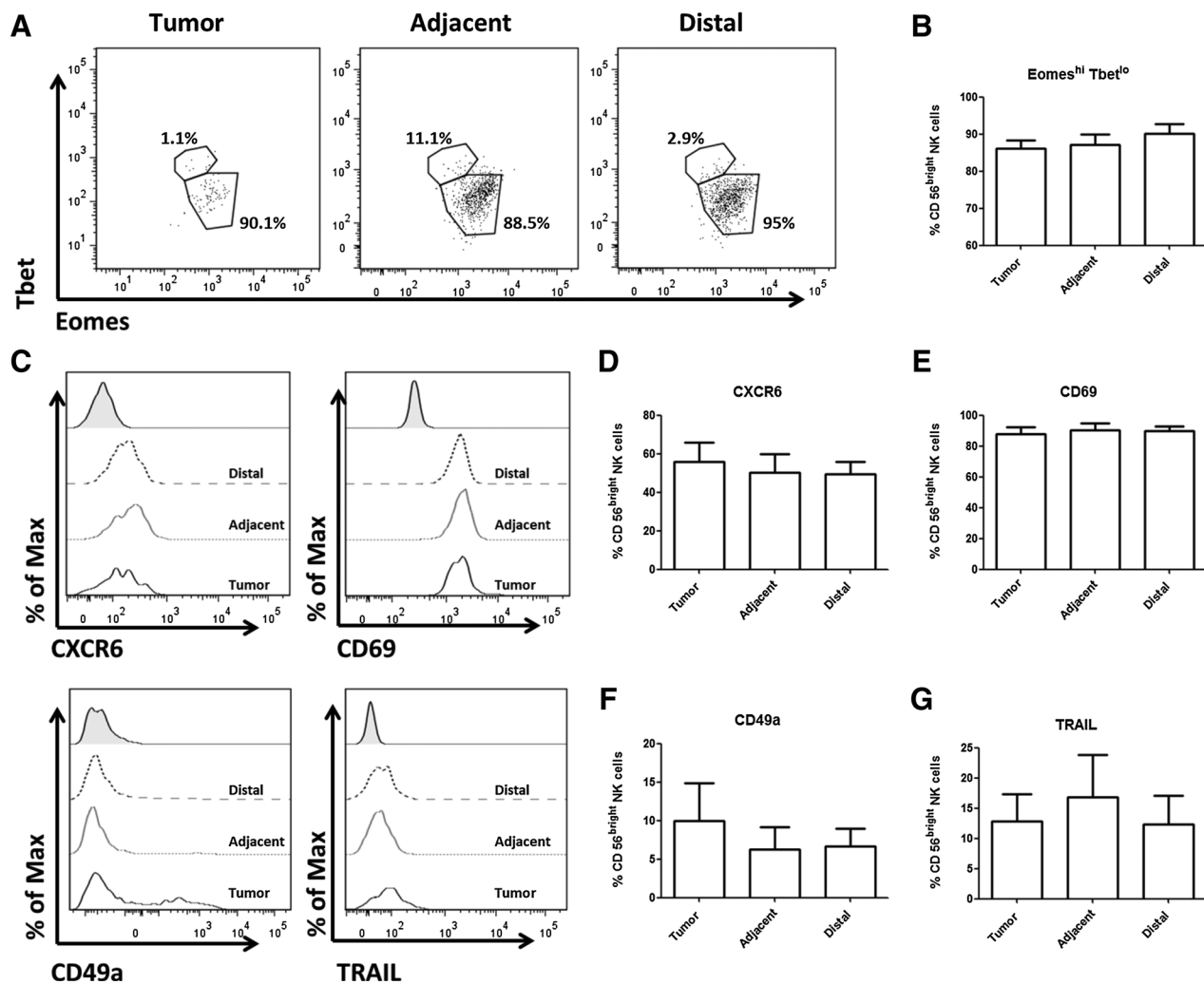
Harmon et al.

**Figure 1.**

Depletion of liver-resident NK cells is evident in CRLM and correlates with CRLM recurrence. Mononuclear cells isolated from tumor, adjacent, and distal tissue samples were stained with monoclonal antibodies. Gating strategy: NK cells were identified from the CD45<sup>+</sup> lymphocyte gate as CD56<sup>+</sup>CD3<sup>-</sup>. We then gated CD56<sup>bright</sup>CD16<sup>-/+</sup> and CD56<sup>dim</sup>CD16<sup>+</sup> subsets. T cells were identified as CD3<sup>+</sup>CD56<sup>-</sup> lymphoid cells. Absolute counts were established using 123Count eBeads. **A**, Representative dot plots of lymphoid populations in samples from tumor, adjacent, and distal tissue. **B**, The percentage of NK cells in tumor, adjacent, and distal tissue ( $n = 18$ ). **C**, Absolute counts of NK cells per milligram of tissue from tumor, adjacent, and distal samples ( $n = 9$ ). **D**, Absolute counts of NK cells per milligram of tissue in patients with hepatic recurrence ( $n = 3$ ) and no recurrence ( $n = 6$ ). **E**, The percentage of T cells in tumor, adjacent, and distal tissue ( $n = 18$ ). **F**, Absolute counts of T cells per milligram of tissue from tumor, adjacent, and distal samples ( $n = 9$ ). **G**, Absolute counts of T cells per milligram of tissue in patients with hepatic recurrence ( $n = 3$ ) and no recurrence ( $n = 6$ ). **H**, Representative dot plots of NK-cell subsets in tumor, adjacent, and distal tissue. **I**, CD56<sup>bright</sup>CD16<sup>-/+</sup> NK-cell frequencies in tumor, adjacent, and distal tissue ( $n = 18$ ). **J**, Absolute counts of CD56<sup>bright</sup> NK cells per milligram of tissue from tumor, adjacent, and distal samples ( $n = 9$ ). **K**, Absolute counts of CD56<sup>bright</sup> NK cells per milligram of tissue in patients with hepatic recurrence ( $n = 3$ ) and no recurrence ( $n = 6$ ). Data presented as mean  $\pm$  SEM. Data were analyzed using the Friedman test, with Dunn multiple comparison test (**B**, **C**, **E**, **F**, **I**, **J**) or Mann-Whitney  $U$  test (**D**, **G**, **K**) (\*,  $P < 0.05$ ; \*\*,  $P < 0.01$ ; \*\*\*,  $P < 0.001$ ).

(Supplementary Fig. S2D–H). Tumor-infiltrating liver-resident NK cells displayed increased expression of NKP44 (a marker of NK-cell activation) but no associated increase in activating receptors such as NKG2D, NKp46, or NKG2C (Fig. 3A–E). We next analyzed the expression of cytotoxic molecules in

liver-resident NK cells from tumor-bearing liver. Similar expression of perforin, granzyme A, granzyme B, or granzyme K was observed in each site, indicating that cytotoxic potential was maintained in tumor-infiltrating CD56<sup>bright</sup> NK cells (Fig. 3F–J).

**Figure 2.**

Tumor-infiltrating CD56<sup>bright</sup> NK cells maintain a liver-resident phenotype. **A**, Representative dot plots of Eomes and Tbet expression in CD56<sup>bright</sup> NK cells in samples from tumor, adjacent, and distal tissue. **B**, The percentage of Eomes<sup>hi</sup> Tbet<sup>lo</sup> CD56<sup>bright</sup> NK cells in tumor, adjacent, and distal tissue. **C**, Representative histograms of CXCR6, TRAIL, CD69, and CD49a in CD56<sup>bright</sup> NK cells in samples from tumor (solid line), adjacent (dotted line), and distal tissue (dashed line; black filled bar, FMO). **D**, The percentage of CXCR6<sup>+</sup> CD56<sup>bright</sup> NK cells in tumor, adjacent, and distal tissue. **E**, The percentage of CD69<sup>+</sup> CD56<sup>bright</sup> NK cells in tumor, adjacent, and distal tissue. **F**, The percentage of CD49a<sup>+</sup> CD56<sup>bright</sup> NK cells in tumor, adjacent, and distal tissue. **G**, The percentage of TRAIL<sup>+</sup> CD56<sup>bright</sup> NK cells in tumor, adjacent, and distal tissue. Data presented as mean  $\pm$  SEM. Data were analyzed using the Friedman test, with Dunn multiple comparison test. (**B**,  $n = 6$ ; **D–G**,  $n = 5$ ).

### Liver-resident NK cells undergo apoptosis in the tumor microenvironment

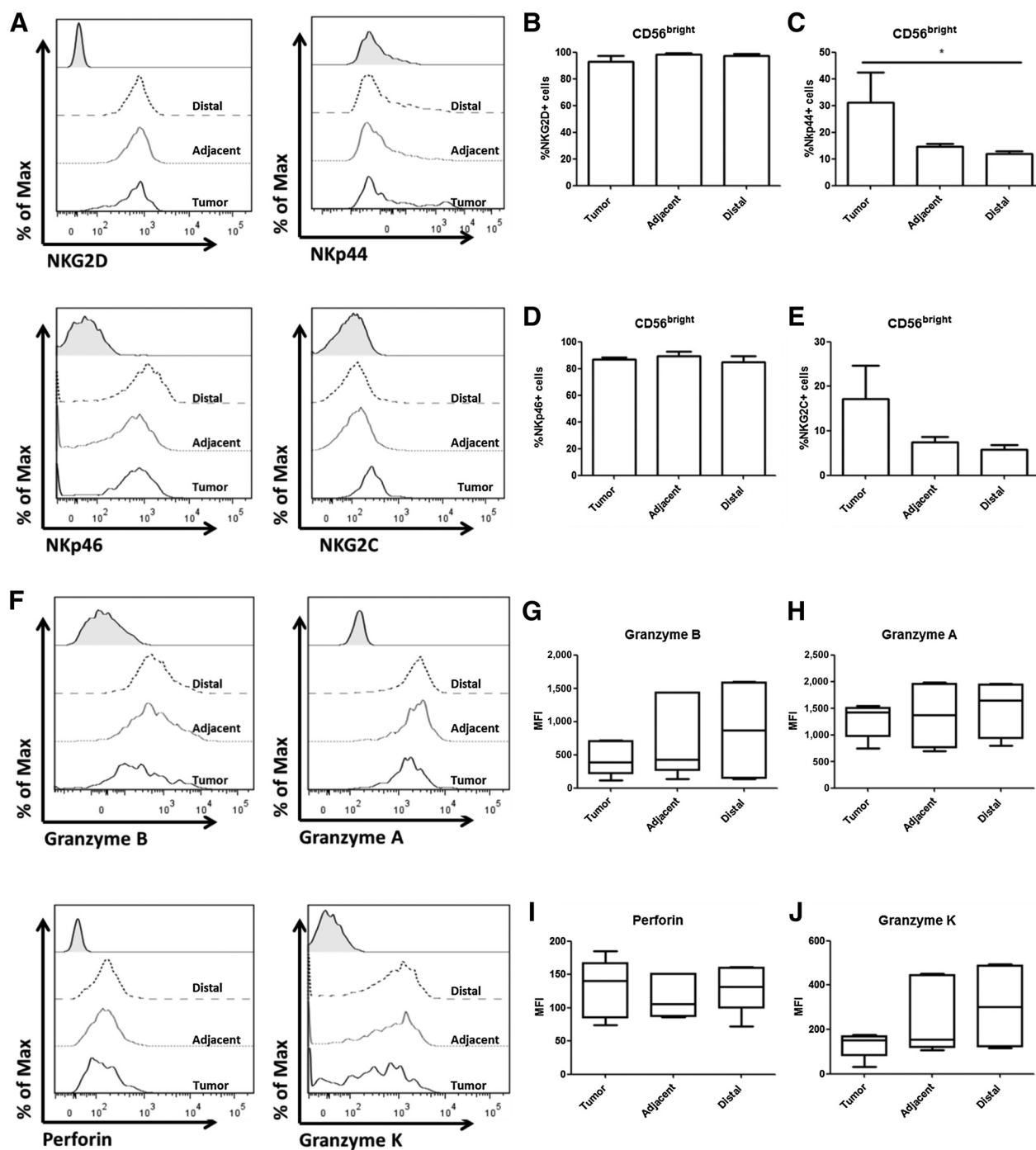
To address the depletion of NK cells from CRLM tumors, we used a CM culture system to identify the mechanism by which CD56<sup>bright</sup> NK cells are lost from tumor tissue. Tumor and donor liver tissue were cultured for 72 hours, and supernatants were used to treat NK-cell subsets isolated from donor liver perfusate. Treatment with CRLM-CM had no effect on the migration ability of the liver-resident NK cells *in vitro* (Supplementary Fig. S3A–S3C). CD56<sup>dim</sup> NK cells had a reduced capacity to migrate toward TCM compared with healthy LCM, possibly accounting for their decreased numbers in CRLM tumors (Supplementary Fig. S3D).

In the absence of a defect in migration, we hypothesized that the tumor microenvironment was inducing apoptosis of liver-resident NK cells. NK-cell subsets from donor liver

perfusate were treated with liver (LCM) and CRLM (TCM) CM for 24 hours. There was a significant increase in the proportion of late apoptotic (Annexin V<sup>+</sup>/7-AAD<sup>+</sup>) liver-resident NK cells treated with TCM compared with LCM but no change in early apoptotic cells (LCM: 21.1%  $\pm$  2.8%, TCM: 39.2%  $\pm$  8.1%,  $P = 0.034$ ; Fig. 4A–C), with no similar increase observed in CD56<sup>dim</sup> NK cells ( $P = 0.92$ ; Fig. 4D and E). The proportion of late apoptotic cells was significantly higher in CD56<sup>bright</sup> NK cells treated with TCM, compared with CD56<sup>dim</sup> cells (Fig. 4F). This apoptosis was not reversible when extrinsic cell signals (i.e., TRAIL, Fas signaling) were blocked through the Caspase 8 inhibitor Z-IETD-FMK ( $P = 0.88$ ; Fig. 4G).

The tumor microenvironment can be inhospitable to immune cells due to the reduced availability of growth factors,

Harmon et al.

**Figure 3.**

Remaining tumor-infiltrating  $CD56^{\text{bright}}$  NK cells are activated and express the proteins required for cytotoxic responses. **A**, Representative histograms of NKG2D, NKp46, NKp44, and NKG2C in  $CD56^{\text{bright}}$  NK cells in samples from tumor (solid line), adjacent (dotted line), and distal tissue (dashed line; black filled bar, FMO). **B**, The percentage of  $NKG2D^+CD56^{\text{bright}}$  NK cells in tumor, adjacent, and distal tissue. **C**, The percentage of  $NKp44^+CD56^{\text{bright}}$  NK cells in tumor, adjacent, and distal tissue. **D**, The percentage of  $NKp46^+CD56^{\text{bright}}$  NK cells in tumor, adjacent, and distal tissue. **E**, The percentage of  $NKG2C^+CD56^{\text{bright}}$  NK cells in tumor, adjacent, and distal tissue. **F**, Representative histograms of granzyme B, perforin, granzyme A, and granzyme K in  $CD56^{\text{bright}}$  NK cells in samples from tumor (solid line), adjacent (dotted line), and distal tissue (dashed line; black filled bar, FMO). **G**, The expression of granzyme B in  $CD56^{\text{bright}}$  NK cells from tumor, adjacent, and distal tissue. **H**, The expression of perforin in  $CD56^{\text{bright}}$  NK cells from tumor, adjacent, and distal tissue. **I**, The expression of granzyme A in  $CD56^{\text{bright}}$  NK cells from tumor, adjacent, and distal tissue. **J**, The expression of granzyme K in  $CD56^{\text{bright}}$  NK cells from tumor, adjacent, and distal tissue. Data presented as mean  $\pm$  SEM. Data analyzed using the Friedman test, with Dunn multiple comparison test ( $n = 5$ ; \*,  $P < 0.05$ ).

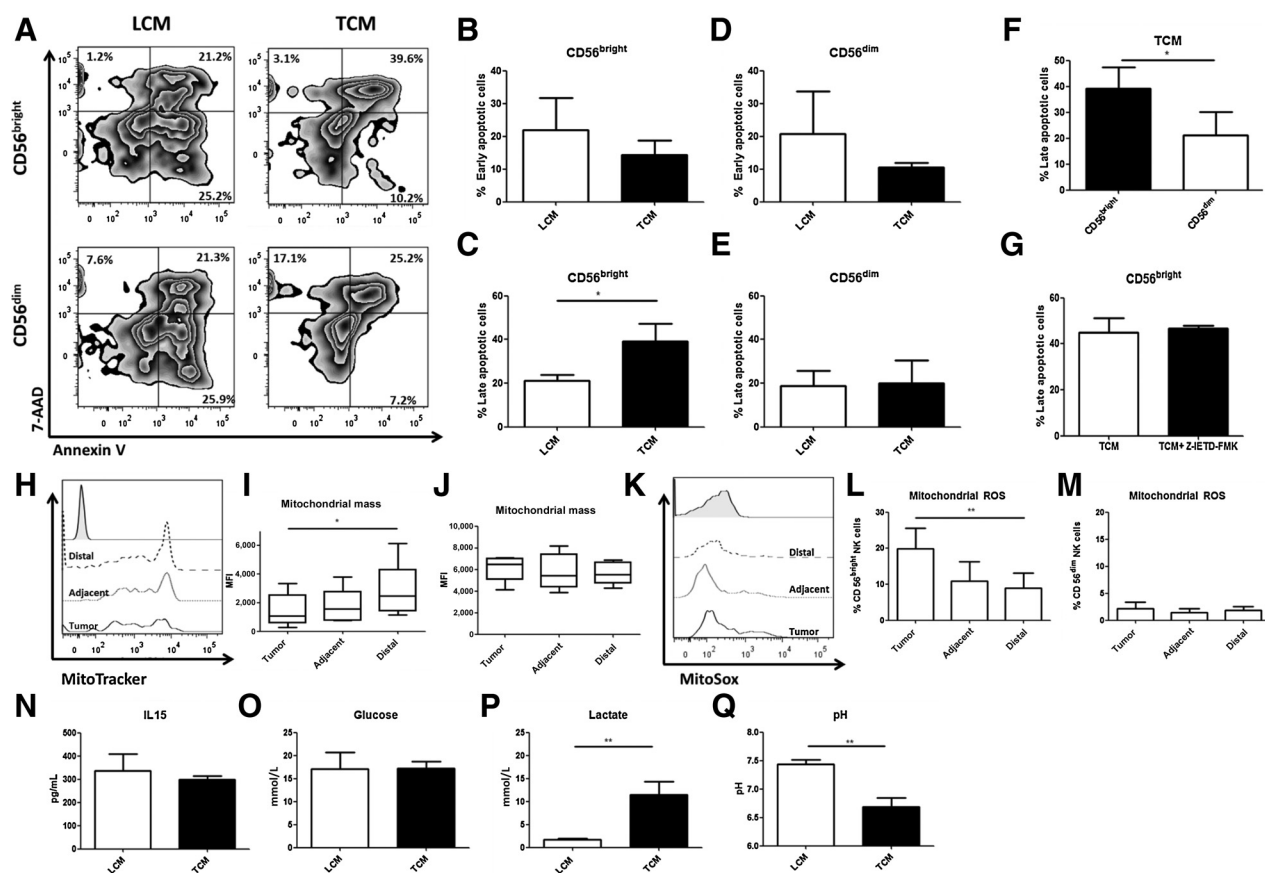


**Figure 4.**

Liver-resident NK cells undergo apoptosis, via intrinsic cell death signaling, associated with elevated lactate in the CRLM tumor microenvironment. Healthy liver-resident NK cells and conventional NK cells were isolated from donor liver perfusate. Cells were cultured with 50% v/v CM from CRLM tumors (TCM) or donor liver biopsies (LCM) for 24 hours. Apoptosis was assessed by annexin V and 7-AAD staining. **A**, Representative dot plots of annexin V/7AAD staining in CD56<sup>bright</sup> and CD56<sup>dim</sup> NK cells after treatment with LCM or CRLM. **B**, Percentage of early apoptotic CD56<sup>bright</sup> NK cells after treatment with LCM or TCM. **C**, Percentage of late apoptotic CD56<sup>bright</sup> NK cells after treatment with LCM or TCM. **D**, Percentage of early apoptotic CD56<sup>dim</sup> NK cells after treatment with LCM or TCM. **E**, Percentage of late apoptotic CD56<sup>dim</sup> NK cells after treatment with LCM or TCM. **F**, Percentage of late apoptotic NK-cell subsets after treatment with TCM. CD56<sup>bright</sup> NK cells were pretreated with caspase 8 inhibitor Z-IETD-FMK for 2 hours before 24 hours of culture. **G**, Percentage of late apoptotic CD56<sup>bright</sup> NK cells after treatment with TCM with/without Z-IETD-FMK. NK cells from tumor-bearing tissue were assessed for evidence of mitochondrial stress. **H**, Representative histograms of MitoTracker in CD56<sup>bright</sup> NK cells in samples from tumor (solid line), adjacent (dotted line), and distal tissue (dashed line; black filled bar, FMO). **I**, MitoTracker staining in CD56<sup>bright</sup> NK cells in tumor, adjacent, and distal tissue. **J**, MitoTracker staining in CD56<sup>dim</sup> NK cells in tumor, adjacent, and distal tissue. **K**, Representative histograms of MitoSox in CD56<sup>bright</sup> NK cells in samples from tumor (solid line), adjacent (dotted line), and distal tissue (dashed line; black filled bar, FMO). **L**, The percentage of MitoSox positive CD56<sup>bright</sup> NK cells in tumor, adjacent, and distal tissue. **M**, The percentage of MitoSox positive CD56<sup>dim</sup> NK cells in tumor, adjacent, and distal tissue. CM from donor livers (LCM) and colorectal liver metastasis (TCM) were generated and analyzed for cytokines and metabolites. **N**, IL15 concentration in LCM and TCM. **O**, Glucose concentration in LCM and TCM. **P**, Lactate concentration in LCM and TCM. **Q**, pH measurement of LCM and TCM. Data presented as mean  $\pm$  SEM. Data were analyzed using Wilcoxon matched pairs test (**B-G**), Mann-Whitney *U* test (**N-P**) or Friedman test, with Dunn multiple comparison test (**I-M**). **A-M**,  $n = 5$ ; **N-P**,  $n = 10$ ; \*,  $P < 0.05$ ; \*\*,  $P < 0.01$ .

essential amino acids, and metabolites. We therefore investigated whether liver-resident NK cells showed signs of mitochondrial stress in the CRLM tumor microenvironment. There is a decrease in the mitochondrial mass of CD56<sup>bright</sup> NK cells in CRLM tumors compared with surrounding tissue, which is not seen in tumor-infiltrating CD56<sup>dim</sup> NK cells (Fig. 4H–J). This is accompanied by the production of mitochondrial ROS, which is significantly increased in tumor-infiltrating CD56<sup>bright</sup> NK cells compared with surrounding tissue (Fig. 4K–L). This is not the case with CD56<sup>dim</sup> NK cells, which do not produce mitochondrial ROS (Fig. 4M). Mitochondrial mass is significantly lower in liver-resident NK cells compared with CD56<sup>dim</sup> NK cells in liver perfusate (Supplementary Fig. S4A and B),

suggesting an intrinsic difference in metabolic activity may underpin the sensitivity of liver-resident CD56<sup>bright</sup> NK cells to apoptosis.

We next attempted to identify the factor responsible for inducing mitochondrial stress in tumor-infiltrating NK cells. NK cells are dependent on IL15 for survival, and withdrawal of this growth factor can cause mitochondrial dysfunction. However, in supernatant from CRLM, IL15 was detected at similar concentrations to donor tissue (TCM:  $335.6 \pm 74$  pg/mL, LCM:  $300 \pm 15.4$  pg/mL,  $P = 0.84$ ; Fig. 4N). Availability of glucose in the tumor microenvironment can also be a rate-limiting step in immune activation and survival; however, in this *in vitro* system glucose did not differ between the LCM and

Harmon et al.

TCM but may play a greater role *in vivo* (TCM:  $17.1 \pm 3.6$  mmol/L, LCM:  $17.2 \pm 1.5$  mmol/L,  $P = 0.49$ ; Fig. 4O). Furthermore, expression of glucose transporter (GLUT1), amino acid transporter (CD98), and transferrin receptor (CD71) did not differ between donor NK-cell subsets and was unchanged in tumor-infiltrating CD56<sup>bright</sup> NK cells, which indicates nutrient availability may not be drastically altered (Supplementary Fig. S5A–H). Despite comparable concentrations of glucose, CRLM tumors appeared more glycolytically active compared with nontumor tissue, producing significantly higher concentrations of lactate (TCM:  $11.5 \pm 2.8$  mmol/L (range, 1.59–24.9 mmol/L), LCM:  $1.7 \pm 0.3$  mmol/L,  $P = 0.002$ ; Fig. 4P) and increased expression of *GLUT1* mRNA in tumor samples compared with adjacent tissue, as well as increased expression of the lactate transporter *SLC16A3* (Supplementary Fig. S6A–S6C). This increased production of lactate led to a significant decrease in the

pH of CM (TCM: pH  $6.6 \pm 0.16$ , LCM: pH  $7.4 \pm 0.08$ ,  $P = 0.0043$ ; Fig. 4Q).

#### Tumor-derived lactic acid induces ROS-mediated apoptosis of CD56<sup>bright</sup> NK cells

We used two forms of lactate to investigate its effect on donor liver-resident NK cells, sodium lactate (basic form), and lactic acid (acidic form) at 10 and 20 mmol/L. No significant change was observed in the proportion of early apoptotic NK cells under any condition tested (Supplementary Fig. S7A–S7G). Sodium lactate did not induce an increase in late apoptotic cells in either CD56<sup>bright</sup> or CD56<sup>dim</sup> NK cells (Fig. 5A and B). Lactic acid induced a significant increase in late apoptotic CD56<sup>bright</sup> NK cells (media:  $13.5\% \pm 2.8\%$ , 10 mmol/L lactic acid:  $20.7\% \pm 4.6\%$ , 20 mmol/L lactic acid:  $43.4\% \pm 9.1\%$ ,  $P = 0.01$ ; Fig. 5C) but not in CD56<sup>dim</sup> NK cells (Fig. 5D). In order to determine if this process was pH mediated, medium was altered to pH 7.4

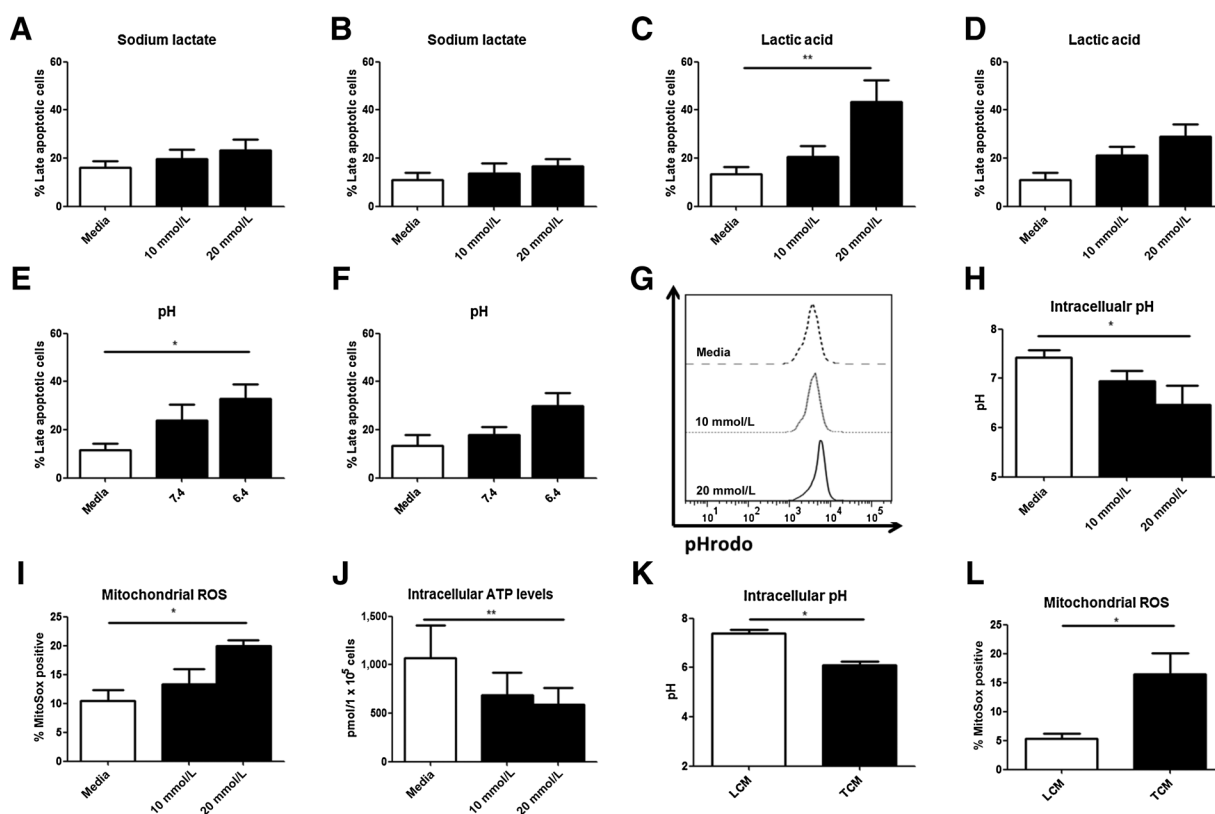


**Figure 5.**

Lactic acid induces apoptosis of liver-resident NK cells by reducing intracellular pH resulting in the accumulation of mitochondrial ROS. Healthy liver-resident NK cells and conventional NK cells were isolated from donor liver perfusate. Cells were cultured for 24 hours in the presence of 10 or 20 mmol/L sodium lactate or lactic acid or media with pH 7.4 or 6.4. Apoptosis was assessed by annexin V and 7-AAD staining. **A**, Percentage of late apoptotic CD56<sup>bright</sup> NK cells after treatment with sodium lactate. **B**, Percentage of late apoptotic CD56<sup>dim</sup> NK cells after treatment with sodium lactate. **C**, Percentage of late apoptotic CD56<sup>bright</sup> NK cells after treatment with lactic acid. **D**, Percentage of late apoptotic CD56<sup>dim</sup> NK cells after treatment with lactic acid. **E**, Percentage of late apoptotic CD56<sup>bright</sup> NK cells after culture in media pH 7.4 or 6.4. **F**, Percentage of late apoptotic CD56<sup>dim</sup> NK cells after culture in media pH 7.4 or 6.4. CD56<sup>bright</sup> NK cells were cultured for 2 hours in the presence of 10 or 20 mmol/L lactic acid. **G**, Representative histogram of pHrodo staining in CD56<sup>bright</sup> cultured in media (dashed line), 10 mmol/L lactic acid (dotted line), or 20 mmol/L lactic acid (solid line). **H**, Intracellular pH of CD56<sup>bright</sup> cells cultured in media, 10 mmol/L lactic acid, or 20 mmol/L lactic acid. **I**, Percentage of MitoSox-positive CD56<sup>bright</sup> cells cultured in media, 10 mmol/L lactic acid, or 20 mmol/L lactic acid. **J**, Concentration of ATP in CD56<sup>bright</sup> NK cells cultured in media, 10 mmol/L lactic acid, or 20 mmol/L lactic acid. CD56<sup>bright</sup> NK cells were cultured for 2 hours in the presence of LCM or TCM. **K**, Intracellular pH of CD56<sup>bright</sup> cells cultured in LCM or TCM. **L**, Percentage of MitoSox-positive CD56<sup>bright</sup> cells cultured in LCM or TCM. Data presented as mean  $\pm$  SEM. Data were analyzed using Friedman test, with Dunn multiple comparison test (**A–J**), or Mann–Whitney *U* test (**K–L**).  $n = 5$ ; \*,  $P < 0.05$ ; \*\*,  $P < 0.01$ .

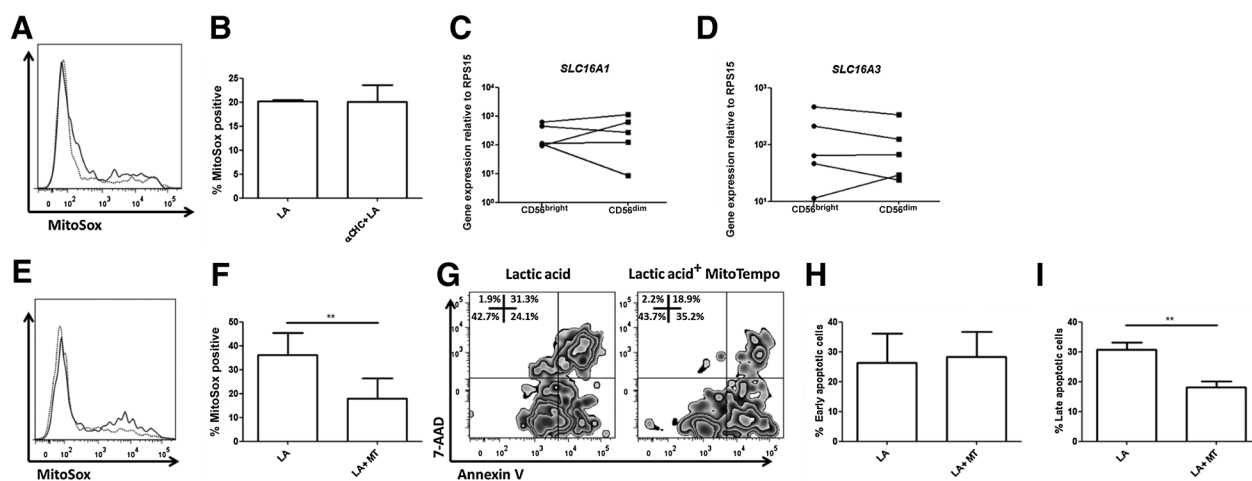


**Figure 6.**

Lactic acid induced apoptosis of liver-resident NK cells can be prevented by treatment with ROS scavenger MitoTempo. Healthy liver-resident NK cells were isolated from donor liver perfusate and pretreated with a lactate transport inhibitor ( $\alpha$ CHC, 500  $\mu$ mol/L) or ROS scavenger (MitoTempo, 50  $\mu$ mol/L) for 2 hours. Lactic acid was then added to cultures at 20 mmol/L for 2 or 24 hours. **A**, Representative histogram of MitoSox staining in CD56<sup>bright</sup> cultured in lactic acid 20 mmol/L (solid line) or  $\alpha$ CHC and 20 mmol/L lactic acid (dotted line). **B**, Percentage of MitoSox<sup>+</sup> CD56<sup>bright</sup> cells cultured in 20 mmol/L lactic acid or  $\alpha$ CHC and 20 mmol/L lactic acid ( $n = 3$ ). Real-time PCR was performed on sorted NK subsets from liver perfusate. Gene expression was normalized to internal control *RPS15*. **C**, Expression of *SLC16A1* (MCT1) in CD56<sup>bright</sup> and CD56<sup>dim</sup> NK cells. **D**, Expression of *SLC16A3* (MCT4) in CD56<sup>bright</sup> and CD56<sup>dim</sup> NK cells ( $n = 5$ ). **E**, Representative histogram of MitoSox staining in CD56<sup>bright</sup> lactic acid 20 mmol/L (solid line) or MitoTempo and 20 mmol/L lactic acid (dotted line). **F**, Percentage of MitoSox-positive CD56<sup>bright</sup> cells cultured in lactic acid 20 mmol/L or MitoTempo and 20 mmol/L lactic acid ( $n = 5$ ). **G**, Representative dot plot of annexin V/7-AAD staining in CD56<sup>bright</sup> NK cells treated with lactic acid 20 mmol/L or MitoTempo and 20 mmol/L lactic acid. **H**, Percentage of early apoptotic CD56<sup>bright</sup> cells cultured in lactic acid 20 mmol/L or MitoTempo and 20 mmol/L lactic acid. **I**, Percentage of late apoptotic CD56<sup>bright</sup> cells cultured in lactic acid 20 mmol/L or MitoTempo and 20 mmol/L lactic acid ( $n = 5$ ). Data presented as mean  $\pm$  SEM. Data were analyzed using the Wilcoxon matched pairs test. \*\*,  $P < 0.01$ .

and 6.4 to mimic the pH of normal tissue and tumor tissue with 20 mmol/L lactic acid. Liver-resident CD56<sup>bright</sup> NK cells undergo significantly higher frequency of apoptosis in pH 6.4 (media: 11.5%  $\pm$  2.7%, pH 7.4: 23.9%  $\pm$  6.5%, pH 6.4: 32.9%  $\pm$  5.9%,  $P = 0.041$ ; Fig. 5E). Apoptosis did increase in CD56<sup>dim</sup> NK cells; however, this was not statistically significant (Fig. 5F). Although there appears to be a trend toward increased apoptosis in CD56<sup>dim</sup> NK cells treated with lactic acid and low pH media, this was not significant and highlights the increased susceptibility of liver-resident CD56<sup>bright</sup> NK cells to these environments.

In order to determine the mechanism by which CD56<sup>bright</sup> NK cells undergo apoptosis, donor liver-resident NK cells were treated with lactic acid for 2 hours at 10 and 20 mmol/L. After 2 hours, the intracellular pH of NK cells decreases significantly (media: pH 7.4  $\pm$  0.15, 10 mmol/L lactic acid: pH 6.9  $\pm$  0.2, 20 mmol/L lactic acid: pH 6.5  $\pm$  0.4,  $P = 0.0046$ ; Fig. 5G and H). This was accompanied by an increase in mitochondrial ROS production, similar to that seen in NK from CRLM tumor samples (media: 10.4%  $\pm$  1.9%, 10 mmol/L lactic acid: 13.3%  $\pm$  2.6%, 20 mmol/L lactic acid: 20.0%  $\pm$  0.9%,  $P = 0.021$ ; Fig. 5I). In addition, intracellular ATP dropped significantly in lactic acid-treated cells (media: 1070  $\pm$  334 pmol/10<sup>5</sup> cells, 10 mmol/L lactic acid: 688  $\pm$  230 pmol/10<sup>5</sup> cells, 20 mmol/L lactic acid: 589  $\pm$  178 pmol/10<sup>5</sup> cells,  $P = 0.008$ ; Fig. 5J). Furthermore, when liver-resident NK cells were treated with TCM for 2 hours, a decrease in intracellular pH was observed (TCM: pH 6.1  $\pm$  0.15, LCM: pH 7.38  $\pm$  0.16,  $P = 0.018$ ; Fig. 5K), accompanied by the production of mitochondrial ROS (TCM: 16.5%  $\pm$  3.5%, LCM: 5.3%  $\pm$  0.86%,  $P = 0.037$ ; Fig. 5L). Together, these results

indicate that lactic acid in the tumor microenvironment causes pH-dependent mitochondrial stress and metabolic dysfunction, which promotes apoptosis.

#### Liver-resident NK-cell apoptosis is ROS mediated but does not require lactate transport

We next attempted to block lactate transport using  $\alpha$ -cyano-4-hydroxycinnamic acid ( $\alpha$ CHC). However, pretreatment with  $\alpha$ CHC did not reduce mitochondrial ROS production after exposure to lactic acid (Fig. 6A and B). Furthermore, NK-cell subsets do not differ in their expression of lactate transporters *SLC16A1* or *SLC16A3* (Fig. 6C and D). These results indicate that the effects of lactic acid were independent of transport into the cell and are more likely related to changes in the pH of the microenvironment.

In order to determine whether NK-cell apoptosis was ROS mediated, we utilized MitoTempo, a mitochondria-specific ROS scavenger. Treatment with MitoTempo significantly reduced mitochondrial ROS (lactic acid: 36.1%  $\pm$  9.3%, lactic acid + MitoTempo: 18.0%  $\pm$  8.5%,  $P = 0.002$ ; Fig. 6E and F) and rescued liver-resident NK cells from apoptosis after 24-hour treatment with lactic acid, decreasing the proportion of late apoptotic cells (lactic acid: 30.7%  $\pm$  2.5%, lactic acid + MitoTempo: 18.1%  $\pm$  2.0%,  $P = 0.0013$ ; Fig. 6G–I).

## Discussion

In this study, we have characterized the NK-cell repertoire of tumor-bearing liver in patients with CRLM and demonstrated a significant depletion of liver-resident NK cells from CRLM tumors. We have evidence that NK-cell depletion correlates with

CRLM recurrence. This depletion is induced by an accumulation of lactate in the tumor microenvironment, causing a reduction in intracellular pH in hepatic NK cells, leading to mitochondrial dysfunction and apoptosis.

NK cells are essential components of the hepatic antitumor immune repertoire. Liver NK cells have been shown to be cytotoxic against tumor cells and should provide the liver with ample antitumor immunity (33–35). The liver-resident NK-cell subpopulation displays increased expression of cytotoxicity receptors, expresses cytotoxic molecules, and is capable of similar direct cytotoxicity against SW620 cells, compared with conventional NK cells. Furthermore, TRAIL expression was significantly increased throughout the tumor-bearing liver, indicating that NK-cell immunosurveillance is heightened in CRLM.

Previous reports have been contradictory, with one claiming that the presence of NK cells in CRLM is correlated with a reduced life expectancy (36) and another with improved disease outcome (20). However, specific NK-cell subsets were not investigated in either of these studies, perhaps accounting for the opposing conclusions. Here, we have identified a significant reduction in liver-resident NK cells from CRLM tumors, despite effective migration toward CRLM-CM. This depletion correlated with hepatic recurrence postresection. This finding parallels results from primary colorectal cancer tumors, which are relatively devoid of NK cells, with surrounding tissue containing normal frequencies of NK-cell populations (21).

We hypothesized that NK cells undergo apoptosis after migration into the tumor microenvironment. *Ex vivo* tumor-infiltrating CD56<sup>bright</sup> NK cells displayed increased mitochondrial ROS production and decreased mitochondrial mass compared with cells from surrounding tissue and infiltrating CD56<sup>dim</sup> NK cells. CRLM tumors appear highly glycolytic, with higher *GLUT1* expression, lactate transporters, and extracellular lactate. Lactate is produced by tumor cells during Warburg metabolism and is then exported via monocarboxylate transporters (MCT1/4) along with protons, lowering the extracellular pH (26). *In vitro*, lactic acid induced significant apoptosis of liver-resident NK cells. The acidic environment provoked a change in intracellular pH of liver-resident NK cells, production of mitochondrial ROS, and reduced ATP generation, inducing intrinsic ROS-mediated apoptosis. Lactate is a potent immune modulator in the tumor microenvironment, known to polarize macrophages and neutrophils, suppress DC activity, and dysregulate and kill T and NK cells (29, 37–40), and our results implicate lactate as the intrinsic cell death signal for liver-resident NK cells. Mechanistically, our results are similar to that described in murine NK cells in a metastatic B16 melanoma model by Brand and colleagues (29), and our results extend on this work to illustrate how a ROS scavenger (MitoTempo) is able to mitigate the effect of pH-induced damage and prevent apoptosis in human tissue-resident NK cells. This result highlights the potential of targeting lactate and the microenvironment pH in order to treat metastatic malignancies in humans.

Reasons for increased liver-resident NK-cell susceptibility to pH induced cellular stress compared with CD56<sup>dim</sup> NK cells are unknown. Lymphocytes have been shown to be capable of maintaining intracellular pH in acidic conditions to a certain point (~pH 6.8; ref. 41). HCO<sup>-</sup> provides most of the buffering capacity in the cell and is produced from CO<sub>2</sub> generated from mitochondrial respiration (42). Cells with greater mitochondrial mass and an active TCA cycle produce more CO<sub>2</sub> and have greater buffering capacity. We have shown that liver-resident NK

cells have significantly lower mitochondrial mass, and increased mitochondrial ROS production, compared with CD56<sup>dim</sup> NK cells, reducing their capacity to generate CO<sub>2</sub>, possibly making them more susceptible to extracellular pH changes.

The recurrence of CRLM after successful resection occurs in up to 70% of patients. Evidently, immune surveillance mechanisms in the liver remain compromised after removal of the tumor. We found that disease recurrence correlates with reduced NK-cell numbers in CRLM tumors, more so than T cells in the intestine, which predict colorectal cancer outcome (17, 18). Treatment targeting lactate production may benefit these patients, improving immune surveillance in the liver and limiting future tumor growth. We believe this approach will substantially reduce the recurrence rate after surgical resection.

Targeting metabolic pathways in oncology is not a new therapeutic concept, and the use of antimetabolites such as methotrexate, folic acid, or 5-fluorouracil is a common treatment for many cancers, despite their toxicity (43). A lactate-mediated mechanism, by which CRLM subverts local antitumor immunity, provides new opportunities for therapies that target specific metabolic pathways. Inhibition of glycolysis in tumor cells is of growing interest to oncologists; however, identifying components in this pathway that specifically inhibit tumor growth and spare immune cells is challenging. In preclinical testing, drugs that target GAPDH (Koningic acid) and LDH (FX11) are effective in limiting tumor growth (43–45). The use of systemic bicarbonate buffering, which neutralizes tumor acidity, has been reported to reduce tumor invasiveness and improve NK-cell responses (46, 47); however, patient adherence to treatment can prove difficult. Alternatively, lactate transport can be targeted specifically (AZD3965, NCT01791595) to prevent release of lactate from tumor cells, increasing it to toxic concentrations within tumor cells, reducing their growth, and inducing their apoptosis (48–50).

Our results highlight the immunosurveillance role of liver-resident NK cells, which are depleted in patients with recurrent CRLM. This depletion is driven by tumor-derived lactate, identifying a potential immunometabolic therapeutic target in patients with CRLM. Therapies capable of reducing lactate concentrations within the tumor microenvironment may restore liver-resident NK-cell populations, benefiting patients with both resectable CRLM and inoperable CRLM, by reducing tumor growth and restoring local tumor immunity. We believe this approach could substantially reduce the recurrence rate after surgical resection.

#### Disclosure of Potential Conflicts of Interest

No potential conflicts of interest were disclosed.

#### Authors' Contributions

**Conception and design:** C. Harmon, M.W. Robinson, C. O'Farrelly  
**Development of methodology:** C. Harmon, M.W. Robinson, L. Lynch  
**Acquisition of data (provided animals, acquired and managed patients, provided facilities, etc.):** C. Harmon, F. Hand, K. Mentor, E. Hoti, J. Geoghegan, C. O'Farrelly  
**Analysis and interpretation of data (e.g., statistical analysis, biostatistics, computational analysis):** C. Harmon, M.W. Robinson, L. Lynch  
**Writing, review, and/or revision of the manuscript:** C. Harmon, M.W. Robinson, F. Hand, D.D. Houlihan, C. O'Farrelly  
**Administrative, technical, or material support (i.e., reporting or organizing data, constructing databases):** D. Almuaili, C. O'Farrelly  
**Study supervision:** M.W. Robinson, C. O'Farrelly

## Acknowledgments

We wish to thank donor families for participating in this research project. The support of the whole liver transplant team at St. Vincent's University Hospital is gratefully acknowledged. The authors would also like to thank all members of the Comparative Immunology Group for helpful discussion. This work was supported by grants from the Health Research Board of Ireland (RP 2008/189) and a Science Foundation Ireland Investigator Award (12/IA/1667).

## References

1. Ferlay J, Soerjomataram I, Dikshit R, Eser S, Mathers C, Rebelo M, et al. Cancer incidence and mortality worldwide: sources, methods and major patterns in GLOBOCAN 2012. *Int J Cancer* 2015;136:E359–86.
2. Hagggar F, Boushey R. Colorectal cancer epidemiology: incidence, mortality, survival, and risk factors. *Clin Colon Rectal Surg* 2009;22:191–7.
3. Nathan H, de Jong MC, Pulitano C, Ribero D, Strub J, Mentha G, et al. Conditional survival after surgical resection of colorectal liver metastasis: an international multi-institutional analysis of 949 patients. *J Am Coll Surg* 2010;210:755–64, 764–6.
4. Disibio G, French SW. Metastatic patterns of cancers: results from a large autopsy study. *Arch Pathol Lab Med* 2008;132:931–9.
5. Riihimäki M, Hemminki A, Sundquist J, Hemminki K. Patterns of metastasis in colon and rectal cancer. *Sci Rep* 2016;6:1–9.
6. Norris S, Collins C, Doherty DG, Smith F, McEntee G, Traynor O, et al. Resident human hepatic lymphocytes are phenotypically different from circulating lymphocytes. *J Hepatol* 1998;28:84–90.
7. Hata K, Van Thiel DH, Herberman RB, Whiteside TL. Natural killer activity of human liver-derived lymphocytes in various liver diseases. *Hepatology* 1991;14:495–503.
8. Kurioka A, Walker LJ, Klenerman P, Willberg CB. MAIT cells: new guardians of the liver. *Clin Transl Immunol* 2016;5:e98.
9. Kenna T, Golden-Mason L, Norris S, Hegarty JE, O'Farrelly C, Doherty DG. Distinct subpopulations of gamma delta T cells are present in normal and tumor-bearing human liver. *Clin Immunol* 2004;113:56–63.
10. Kenna T, Golden-Mason L, Porcelli Sa, Koezuka Y, Hegarty JE, O'Farrelly C, et al. NKT cells from normal and tumor-bearing human livers are phenotypically and functionally distinct from murine NKT cells. *J Immunol* 2003;171:1775–9.
11. Shuai Z, Leung MW, He X, Zhang W, Yang G, Leung PS, et al. Adaptive immunity in the liver. *Cell Mol Immunol* 2016;13:354–68.
12. Krasnova Y, Putz EM, Smyth MJ, Souza-Fonseca-Guimaraes F. Bench to bedside: NK cells and control of metastasis. *Clin Immunol* 2015;177:50–9.
13. Adotevi O, Godet Y, Galaine J, Lakkis Z, Idreine I, Certoux JM, et al. In situ delivery of allogeneic natural killer cell (NK) combined with cetuximab in liver metastases of gastrointestinal carcinoma: a phase I clinical trial. *Oncoimmunology* 2018;7:e1424673.
14. Harmon C, Robinson MW, Fahey R, Whelan S, Houlihan DD, Geoghegan J, et al. Tissue-resident Eomes hi T-bet lo CD56 bright NK cells with reduced proinflammatory potential are enriched in the adult human liver. *Eur J Immunol* 2016;46:2111–20.
15. Stegmann KA, Robertson F, Hansi N, Gill U, Pallant C, Christophides T, et al. CXCR6 marks a novel subset of T-bet lo Eomes hi natural killer cells residing in human liver. *Sci Rep* 2016;6:26157.
16. Aw Yeang HX, Piersma SJ, Lin Y, Yang L, Malkova ON, Miner C, et al. Cutting edge: human CD49e– NK cells are tissue resident in the liver. *J Immunol* 2017. doi: 10.4049/jimmunol.1601818.
17. Galon J, Costes A, Sanchez-Cabo F, Kirilovsky A, Mlecnik B, Lagorce-Pagès C, et al. Type, density, and location of immune cells within human colorectal tumors predict clinical outcome. *Science* 2006;313:1960–4.
18. Anitei M-G, Zeitoun G, Mlecnik B, Marliot F, Haicheur N, Tosi AM, et al. Prognostic and predictive values of the immunoscore in patients with rectal cancer. *Clin Cancer Res* 2014;20:1891–9.
19. Galon J, Mlecnik B, Bindea G, Angell HK, Berger A, Lagorce C, et al. Towards the introduction of the 'Immunoscore' in the classification of malignant tumors. *J Pathol* 2014;232:199–209.
20. Donadon M, Hudspeth K, Cimino M, Di Tommaso L, Preti M, Tentorio P, et al. Increased infiltration of natural killer and T cells in colorectal liver metastases improves patient overall survival. *J Gastrointest Surg* 2017;21:1226–36.
21. Halama N, Braun M, Kahlert C, Spille A, Quack C, Rahbari N, et al. Natural killer cells are scarce in colorectal carcinoma tissue despite high levels of chemokines and cytokines. *Clin Cancer Res* 2011;17:678–89.
22. Jobin G, Rodriguez-Suarez R, Betito K. Association between natural killer cell activity and colorectal cancer in high-risk subjects undergoing colonoscopy. *Gastroenterology* 2017;153:980–7.
23. Kelly AM, Golden-Mason L, Traynor O, Geoghegan J, McEntee G, Hegarty JE, et al. Changes in hepatic immunoregulatory cytokines in patients with metastatic colorectal carcinoma: implications for hepatic anti-tumor immunity. *Cytokine* 2006;35:171–9.
24. Hand F, Harmon C, Elliott LA, Caiazza F, Lavelle A, Maguire D, et al. Depleted polymorphonuclear leukocytes in human metastatic liver reflect an altered immune microenvironment associated with recurrent metastasis. *Cancer Immunol Immunother* 2018;67:1041–52.
25. Kelly AM, Golden-Mason L, McEntee G, Traynor O, Doherty DG, Hegarty JE, et al. Interleukin 12 (IL-12) is increased in tumor bearing human liver and expands CD8(+) and CD56(+) T cells in vitro but not in vivo. *Cytokine* 2004;25:273–82.
26. Pavlova NN, Thompson CB. The emerging hallmarks of cancer metabolism. *Cell Metab* 2016;23:27–47.
27. Keating SE, Zaiatz-Bittencourt V, Loftus RM, Keane C, Brennan K, Finlay DK, et al. Metabolic reprogramming supports IFN- $\gamma$  production by CD56bright NK cells. *J Immunol* 2016;196:2552–60.
28. Assmann N, O'Brien KL, Donnelly RP, Dyck L, Zaiatz-Bittencourt V, Loftus RM, et al. Srebp-controlled glucose metabolism is essential for ure functional responses. *Nat Immunol* 2017;18:1197–206.
29. Brand A, Singer K, Koehl GE, Koltitz M, Schoenhammer G, Thiel A, et al. LDHA-associated lactic acid production blunts tumor immunosurveillance by T and NK Cells. *Cell Metab* 2016;24:657–71.
30. Kelly A, Fahey R, Fletcher JM, Keogh C, Carroll AG, Siddachari R, et al. CD141 + myeloid dendritic cells are enriched in healthy human liver. *J Hepatol* 2014;60:135–42.
31. Norris S, Doherty DG, Curry MP, McEntee G, Traynor O, Hegarty JE, et al. Selective reduction of natural killer cells and T cells expressing inhibitory receptors for MHC class I in the livers of patients with hepatic malignancy. *Cancer Immunol Immunother* 2003;52:53–8.
32. O'Toole A, Michielsens AJ, Nolan B, Tosetto M, Sheahan K, Mulcahy HE, et al. Tumor microenvironment of both early- and late-stage colorectal cancer is equally immunosuppressive. *Br J Cancer* 2014;111:927–32.
33. Ishiyama K, Ohdan H, Ohira M, Mitsuta H, Arihiro K, Asahara T. Difference in cytotoxicity against hepatocellular carcinoma between liver and periphery natural killer cells in humans. *Hepatology* 2006;43:362–72.
34. Zhang Z, Zhang S, Zou Z, Shi J, Zhao J, Fan R, et al. Hypercytolytic activity of hepatic natural killer cells correlates with liver injury in chronic hepatitis B patients. *Hepatology* 2011;53:73–85.
35. Peng H, Wisse E, Tian Z. Liver natural killer cells: subsets and roles in liver immunity. *Cell Mol Immunol* 2016;13:328–36.
36. Pugh SA, Harrison RJ, Primrose JN, Khakoo SI. T cells but not NK cells are associated with a favourable outcome for resected colorectal liver metastases. *BMC Cancer* 2014;14:180.
37. Husain Z, Huang Y, Seth P, Sukhatme VP. Tumor-Derived lactate modifies antitumor immune response: effect on myeloid-derived suppressor cells and NK cells. *J Immunol* 2013;191:1486–95.
38. Colegio OR, Chu N-Q, Szabo AL, Chu T, Rhebergen AM, Jairam V, et al. Functional polarization of tumor-associated macrophages by tumor-derived lactic acid. *Nature* 2014;513:559–63.
39. Fischer K, Hoffmann P, Voelkl S, Meidenbauer N, Ammer J, Edinger M, et al. Inhibitory effect of tumor cell-derived lactic acid on human T cells. *Blood* 2007;109:3812–9.

Harmon et al.

40. Gottfried E. Tumor-derived lactic acid modulates dendritic cell activation and antigen expression. *Blood* 2006;107:2013–21.
41. Deutsch C, Taylor JS, Wilson DF. Regulation of intracellular pH by human peripheral blood lymphocytes as measured by <sup>19</sup>F NMR. *Proc Natl Acad Sci U S A* 1982;79:7944–8. Available from: <http://www.ncbi.nlm.nih.gov/pubmed/6961462>
42. Casey JR, Grinstein S, Orlowski J. Sensors and regulators of intracellular pH. *Nat Rev Mol Cell Biol* 2010;11:50–61.
43. Luengo A, Gui DY, Vander Heiden MG. Targeting metabolism for cancer therapy. *Cell Chem Biol* 2017;24:1161–80.
44. Liberti MV, Dai Z, Wardell SE, Baccile JA, Liu X, Gao X, et al. A predictive model for selective targeting of the Warburg effect through GAPDH inhibition with a natural product. *Cell Metab* 2017;26:648–659.e8.
45. Le A, Cooper CR, Gouw AM, Dinavahi R, Maitra A, Deck LM, et al. Inhibition of lactate dehydrogenase A induces oxidative stress and inhibits tumor progression. *Proc Natl Acad Sci* 2010;107:2037–42.
46. Ibrahim-Hashim A, Abrahams D, Enriquez-Navas PM, Luddy K, Gatenby RA, Gillies RJ. Tris-base buffer: a promising new inhibitor for cancer progression and metastasis. *Cancer Med* 2017;6:1720–9.
47. Pötl J, Roser D, Bankel L, Hömberg N, Geishauser A, Brenner CD, et al. Reversal of tumor acidosis by systemic buffering reactivates NK cells to express IFN- $\gamma$  and induces NK cell-dependent lymphoma control without other immunotherapies. *Int J Cancer* 2017;140:2125–33.
48. Sonveaux P, Copetti T, De Saedeleer CJ, Végran F, Verrax J, Kennedy KM, et al. Targeting the lactate transporter MCT1 in endothelial cells inhibits lactate-induced HIF-1 activation and tumor angiogenesis. *PLoS One* 2012;7:e33418.
49. Payen VL, Hsu MY, Rådecke KS, Wyart E, Vazeille T, Bouzin C, et al. Monocarboxylate transporter MCT1 promotes tumor metastasis independently of its activity as a lactate transporter. *Cancer Res* 2017;77:5591–601.
50. Sonveaux P, Végran F, Schroeder T, Wergin MC, Julien Verrax J, Rabbani ZN, et al. Targeting lactate-fueled respiration selectively kills hypoxic tumor cells in mice. *J Clin Invest* 2008;118:3930–42.

# Cancer Immunology Research

## Lactate-Mediated Acidification of Tumor Microenvironment Induces Apoptosis of Liver-Resident NK Cells in Colorectal Liver Metastasis

Cathal Harmon, Mark W. Robinson, Fiona Hand, et al.

*Cancer Immunol Res* 2019;7:335-346. Published OnlineFirst December 18, 2018.

<b>Updated version</b>	Access the most recent version of this article at: doi: <a href="https://doi.org/10.1158/2326-6066.CIR-18-0481">10.1158/2326-6066.CIR-18-0481</a>
<b>Supplementary Material</b>	Access the most recent supplemental material at: <a href="http://cancerimmunolres.aacrjournals.org/content/suppl/2018/12/18/2326-6066.CIR-18-0481.DC1">http://cancerimmunolres.aacrjournals.org/content/suppl/2018/12/18/2326-6066.CIR-18-0481.DC1</a>

<b>Cited articles</b>	This article cites 49 articles, 11 of which you can access for free at: <a href="http://cancerimmunolres.aacrjournals.org/content/7/2/335.full#ref-list-1">http://cancerimmunolres.aacrjournals.org/content/7/2/335.full#ref-list-1</a>
-----------------------	--

<b>Citing articles</b>	This article has been cited by 1 HighWire-hosted articles. Access the articles at: <a href="http://cancerimmunolres.aacrjournals.org/content/7/2/335.full#related-urls">http://cancerimmunolres.aacrjournals.org/content/7/2/335.full#related-urls</a>
------------------------	---

<b>E-mail alerts</b>	<a href="#">Sign up to receive free email-alerts</a> related to this article or journal.
----------------------	--

<b>Reprints and Subscriptions</b>	To order reprints of this article or to subscribe to the journal, contact the AACR Publications Department at <a href="mailto:pubs@aacr.org">pubs@aacr.org</a> .
-----------------------------------	--

<b>Permissions</b>	To request permission to re-use all or part of this article, use this link <a href="http://cancerimmunolres.aacrjournals.org/content/7/2/335">http://cancerimmunolres.aacrjournals.org/content/7/2/335</a> . Click on "Request Permissions" which will take you to the Copyright Clearance Center's (CCC) Rightslink site.
--------------------	--